



**Soil moisture
assimilation time
scales**

C. Draper and R. Reichle

This discussion paper is/has been under review for the journal Hydrology and Earth System Sciences (HESS). Please refer to the corresponding final paper in HESS if available.

The impact of near-surface soil moisture assimilation at subseasonal, seasonal, and inter-annual time scales

C. Draper^{1,2} and R. Reichle¹

¹Global Modeling and Assimilation Office, NASA GSFC, Greenbelt, MD, USA

²Universities Space Research Association, Columbia, MD, USA

Received: 9 July 2015 – Accepted: 24 July 2015 – Published: 17 August 2015

Correspondence to: C. Draper (clara.draper@nasa.gov)

Published by Copernicus Publications on behalf of the European Geosciences Union.

Title Page

Abstract

Introduction

Conclusions

References

Tables

Figures



Back

Close

Full Screen / Esc

Printer-friendly Version

Interactive Discussion



Abstract

Nine years of Advanced Microwave Scanning Radiometer – Earth Observing System (AMSR-E) soil moisture retrievals are assimilated into the Catchment land surface model at four locations in the US. The assimilation is evaluated using the unbiased Mean Square Error (ubMSE) relative to watershed-scale in situ observations, with the ubMSE separated into contributions from the subseasonal (SM_{short}), mean seasonal (SM_{seas}) and inter-annual (SM_{long}) soil moisture dynamics. For near-surface soil moisture, the average ubMSE for Catchment without assimilation was $(1.8 \times 10^{-3} \text{ m}^3 \text{ m}^{-3})^2$, of which 19 % was in SM_{long} , 26 % in SM_{seas} , and 55 % in SM_{short} . The AMSR-E assimilation significantly reduced the total ubMSE at every site, with an average reduction of 33 %. Of this ubMSE reduction, 37 % occurred in SM_{long} , 24 % in SM_{seas} , and 38 % in SM_{short} . For root-zone soil moisture, in situ observations were available at one site only, and the near-surface and root-zone results were very similar at this site. These results suggest that, in addition to the well-reported improvements in SM_{short} , assimilating a sufficiently long soil moisture data record can also improve the model representation of important long term events, such as droughts. The improved agreement between the modeled and in situ SM_{seas} is harder to interpret, given that mean seasonal cycle errors are systematic, and systematic errors are not typically targeted by (bias-blind) data assimilation. Finally, the use of one year subsets of the AMSR-E and Catchment soil moisture for estimating the observation-bias correction (rescaling) parameters is investigated. It is concluded that when only one year of data is available, the associated uncertainty in the rescaling parameters should not greatly reduce the average benefit gained from data assimilation, but locally and in extreme years there is a risk of increased errors.

HESSD

12, 7971–8004, 2015

Soil moisture assimilation time scales

C. Draper and R. Reichle

Title Page

Abstract

Introduction

Conclusions

References

Tables

Figures

⏪

⏩

◀

▶

Back

Close

Full Screen / Esc

Printer-friendly Version

Interactive Discussion



1 Introduction

Remotely sensed near-surface soil moisture observations are typically assimilated using a bias-blind assimilation of observations that have been “bias-corrected” to have the same mean as the model forecast soil moisture (Reichle et al., 2007; Scipal et al., 2008; Bolten et al., 2010). This approach is designed to avoid forcing the model into a regime that is incompatible with its assumed (likely erroneous) structure and parameters, or inadvertently introducing any observation biases into the model, while still allowing the assimilation to correct for random errors in the model forecasts (Reichle and Koster, 2004). Here “random” errors are defined as errors that persist for less than the time scale used to – subjectively – define the bias. Observation-bias correction of remotely sensed soil moisture is usually achieved by rescaling the observations to have the same mean and variance as model forecasts, for example by matching their Cumulative Distribution Functions (CDFs; Reichle and Koster, 2004). Traditionally, the observation rescaling (CDF-matching) parameters are estimated over the maximum available coincident observed and forecast data record (Reichle et al., 2007; Scipal et al., 2008; Draper et al., 2012), so that the rescaled observations will retain a signal of any observation-forecast differences that occurred at time scales shorter than the data record. For a multi-year data record assimilating these rescaled observations could then potentially update the model soil moisture with observed information at sub-seasonal, seasonal, and inter-annual time scales.

The physical processes causing soil moisture errors at the above-mentioned sub-seasonal, seasonal, and inter-annual time scales will be quite different. Most notably, in many locations seasonal scale variability is dominated by the mean seasonal cycle (the annually repeating variability), and any errors in the mean seasonal cycle will be systematic (with causes such as incorrect separation of the soil and vegetation moisture signals from remotely sensed brightness temperatures, or in the land surface model vegetation dynamics). In contrast, variability at subseasonal and inter-annual time scales is rarely dominated by repeating cycles, and is more typically associated

HESSD

12, 7971–8004, 2015

Soil moisture assimilation time scales

C. Draper and R. Reichle

[Title Page](#)

[Abstract](#)

[Introduction](#)

[Conclusions](#)

[References](#)

[Tables](#)

[Figures](#)



[Back](#)

[Close](#)

[Full Screen / Esc](#)

[Printer-friendly Version](#)

[Interactive Discussion](#)



Soil moisture assimilation time scales

C. Draper and R. Reichle

[Title Page](#)

[Abstract](#)

[Introduction](#)

[Conclusions](#)

[References](#)

[Tables](#)

[Figures](#)

[⏪](#)

[⏩](#)

[◀](#)

[▶](#)

[Back](#)

[Close](#)

[Full Screen / Esc](#)

[Printer-friendly Version](#)

[Interactive Discussion](#)



with transient atmospheric forcing events. For example, rapid time scale (daily) soil moisture dynamics are driven by factors such as individual precipitation events and changes in cloud cover, while longer time scale (seasonal-plus) dynamics are driven by changes in the atmospheric supply and demand for moisture (Entin et al., 2000).

5 Soil moisture errors at subseasonal scales could then be caused by factors such as atmospheric noise in remotely sensed data, or errors in the daily meteorology of the model atmospheric forcing, while inter-annual scale errors could be caused by factors such as drift in the remote sensor calibration, or incorrect representation of atmospheric drought conditions in the atmospheric forcing.

10 The systematic nature of errors in the mean seasonal cycle is problematic for data assimilation. Theoretically, (bias-blind) data assimilation is not designed, nor optimized, to correct for systematic errors. More practically, if the systematic differences are not due to model errors (i.e., are caused by observation errors, including representativity errors), then assimilating such information can seriously degrade model performance. Consequently, due to concerns over the accuracy of the seasonal cycle in remotely sensed soil moisture, Drusch et al. (2005) suggested that soil moisture observation-bias correction for data assimilation might be better designed so that the model soil moisture seasonal cycle is retained by the assimilation, as has been done in several more recent studies (Bolten et al., 2010; Yilmaz et al., 2015).

20 In addition to the systematic nature of seasonal errors, the time scale dependence of soil moisture errors may also be more generally problematic for observation rescaling. Even within time scales less than one month, Su and Ryu (2015) showed that the multiplicative (differences in standard deviation) and additive (differences in mean) components of the systematic differences between modeled and remotely sensed soil moisture differ across time scales. They highlight that this lack of stationarity cannot be adequately addressed by using bulk statistics to estimate observation rescaling parameters.

25 To better understand the time scale dependency of near-surface soil moisture assimilation, we have then decomposed modeled, remotely sensed, and in situ soil moisture

Soil moisture assimilation time scales

C. Draper and R. Reichle

[Title Page](#)

[Abstract](#)

[Introduction](#)

[Conclusions](#)

[References](#)

[Tables](#)

[Figures](#)



[Back](#)

[Close](#)

[Full Screen / Esc](#)

[Printer-friendly Version](#)

[Interactive Discussion](#)



into separate time series representing soil moisture dynamics at subseasonal, mean seasonal, and inter-annual time scales. We have used this decomposition to examine the differences between remotely sensed and modeled soil moisture at each time scale, how these difference affect observation rescaling, and how assimilating the remotely sensed observations impacts the model soil moisture at each time scale. The decomposition is achieved by fitting each soil moisture time series with harmonic functions specified to target the mean seasonal cycle (SM_{seas}), and the subseasonal (SM_{short}) and inter-annual (SM_{long}) dynamics.

By fitting the appropriate harmonic functions to each time series, we can separate the total mean square error of each soil moisture time series into contributions from each time scale. This is a much more targeted evaluation of soil moisture dynamics at the specific time scales that can then be linked to physical processes than is usually undertaken. Standard evaluation methods focus on bias-blind metrics, such as the correlation or unbiased Root Mean Square Error (ubRMSE, which is calculated after removing the long term mean difference (Entekhabi et al., 2010b)). Both of these are sensitive to soil moisture time series variability at all time scales. While anomaly correlations (R_{anom}), are also used to exclude the seasonal cycle, this is not done consistently, and does not allow the total error to be broken into contributing time scales. Depending on how the anomalies are calculated, R_{anom} measures subseasonal scale errors (anomalies defined relative to a simple moving average, as in Dorigo et al., 2015), or a combination of inter-annual and subseasonal scale errors (anomalies defined relative to the mean seasonal cycle over multiple years as in Draper et al., 2012).

In the second part of this study, we also explore the impact on the assimilation of using short time periods for observation bias correction. When first introducing CDF-matching to rescale remotely sensed soil moisture prior to assimilation, Reichle and Koster (2004) showed that for Scanning Multi-channel Microwave Radiometer (SMMR) soil moisture observations (1979–1987), reasonable rescaling parameters could be estimated using a single year of data. We repeat their investigation using the more modern Advanced Microwave Scanning Radiometer-Earth Observing System (AMSR-

Soil moisture assimilation time scales

C. Draper and R. Reichle

[Title Page](#)

[Abstract](#)

[Introduction](#)

[Conclusions](#)

[References](#)

[Tables](#)

[Figures](#)



[Back](#)

[Close](#)

[Full Screen / Esc](#)

[Printer-friendly Version](#)

[Interactive Discussion](#)



near-surface soil moisture from Catchment and AMSR-E was evaluated using the 5 cm ARS observations, while the root-zone soil moisture from Catchment was evaluated using the average of the 5–60 cm observations (including only times with data reported for all layers). The ARS root-zone soil moisture was used at Little River only, due to very low observation counts over the study period at the other sites. Given that we will focus on evaluating variance, we have not supplemented the ARS observations with observations from single sensor networks, such as SCAN (Schaefer et al., 2007). Unlike the locally dense in situ measurements from the ARS networks, the variance (and mean) of observations from single sensors cannot be assumed representative of the coarse scale soil moisture from Catchment and AMSR-E.

Level 3 Land Parameter Retrieval (LPRM) X-band AMSR-E near-surface soil moisture retrievals at 0.25° resolution were obtained for the grid cells surrounding each site in Table 1. At X-band the observations relate to a surface layer depth slightly less than 1 cm. Only the descending (1:30 a.m. LT) overpass has been used to avoid possible differences in the climatological statistics of day- and night-time observations. The sites were explicitly selected by ARS to avoid possible radio frequency interference and proximity to permanent open water, and the AMSR-E soil moisture retrievals were screened to remove observations with X-band vegetation optical depth above 0.8.

NASA's Catchment land surface model was run over the 9 km EASE grid cells surrounding each study site, using atmospheric forcing fields from Modern Era Retrospective-Analysis for Research (MERRA; Rienecker et al., 2011) and recently improved soil parameters (De Lannoy et al., 2014). The model initial conditions were first spun-up from January 1993 to January 2002 using a single member without perturbations. The ensemble (including perturbations) was then spun-up from January to October 2002 (see Sect. 2.2 for details of the ensemble). For both the model open loop and data assimilation model output, the ensemble average near-surface (0–5 cm) and root zone (0–100 cm) soil moisture is then reported.

Daily ARS and Catchment time series were generated by sampling each at the approximate time of the descending AMSR-E overpass (1:30 a.m. LT). Initially each time

series spanned the AMSR-E data record, rounded down to nine full years from October 2002 to September 2011, however the Little River root-zone soil moisture observations are not available before January 2004, and were truncated to the seven years from October 2004 to September 2011. Also, there were just 21 ARS observations at Reynolds Creek in the last year of this period, and so the Reynolds Creek time series were truncated to the eight years from October 2002 to September 2010. The ARS and AMSR-E sensors can only measure liquid soil moisture, and all data have been screened out when the Catchment model indicates frozen near-surface conditions. Since the Reynolds Creek site is frozen for an extended period each winter, liquid soil moisture is not well defined there during winter, and the Reynolds Creek time series have then been truncated to remove winter, defined from 1 December to 10 March (the period during which the Catchment surface is continuously frozen for at least three of the eight years of the Reynolds Creek record).

2.2 The assimilation experiments

The assimilation experiments were performed using a one-dimensional bias-blind Ensemble Kalman Filter, with the same set-up and ensemble generation as in Liu et al. (2011). We used CDF-matching (Reichle and Koster, 2004) to rescale the observations prior to each assimilation experiment. The details of the time period used to estimate the observation scaling parameters are given in Sect. 3, before presenting each set of results. The benefits of each assimilation experiment have then been compared to that of the Catchment model open loop ensemble mean, in which the same ensemble generation parameters were used, and no observations were assimilated.

2.3 Decomposition of soil moisture time series

We wish to decompose each soil moisture (SM) time series into separate components representing soil moisture dynamics at the subseasonal (SM_{short}), seasonal (SM_{seas}), and inter-annual (SM_{long}) time scales. Variability in a time series at specific time scales

HESSD

12, 7971–8004, 2015

Soil moisture assimilation time scales

C. Draper and R. Reichle

Title Page

Abstract

Introduction

Conclusions

References

Tables

Figures



Back

Close

Full Screen / Esc

Printer-friendly Version

Interactive Discussion



can be isolated by fitting a function made up of the sum of sinusoidal functions. Formally, for some observed time series, y , the function, \hat{y} , is fit for some selection of integers k_i :

$$\hat{y}(t) = a_0 + \sum_{k=k_1, k_2, \dots} a_k \sin\left(\frac{2\pi kt}{n}\right) + b_k \cos\left(\frac{2\pi kt}{n}\right), \quad (1)$$

where t is the time step and n is the length of the time series. $\frac{2\pi k}{n}$ is the (angular) frequency for a sinusoid completing k cycles over n time steps (i.e., that has frequency k/n per time unit), and \hat{y} for $k = k_i$ is referred to as the k_i th harmonic. a_0 is the mean of y . If the time series is sampled at regular intervals and has no missing data, the sinusoids for individual harmonics are orthogonal and independent of each other. This is the basis for the discrete Fourier transform, which exactly fits Eq. (1) to y using the first $n/2$ harmonics (i.e., $k_i = 1, 2, 3, \dots, n/2$). In this study, we use multiple linear least squares regression to fit Eq. (1) to the soil moisture time series for a sum of harmonic frequencies selected to isolate the variability at each target time scale, as described below.

We define SM_{seas} by fitting Eq. (1) to the soil moisture time series for some combination of the annual harmonic frequencies (i.e., for k/n an integer multiple of 1 yr^{-1}). The frequencies higher than 1 yr^{-1} moderate the shape of \hat{y} to account for differences in the shape of the seasonal cycle from the single sinusoid described by the first harmonic. Typically, only a few annual harmonics are necessary to fit the seasonal cycle of geophysical variables (Scharlemann et al., 2008; Vinnikov et al., 2008). Here we define SM_{seas} to be the sum of the first two harmonics, since fitting additional harmonics did not improve the ability to predict withheld data, following the method of Narapusetty et al. (2009). Note that since the same annual harmonics are repeated each year, we are restricting SM_{seas} to represent only the mean seasonal cycle, and any inter-annual variability at seasonal time scales, such as anomalous vegetation growth in a given year, will be assigned to the subseasonal or inter-annual variability, depending on its temporal characteristics.

Soil moisture assimilation time scales

C. Draper and R. Reichle

[Title Page](#)[Abstract](#)[Introduction](#)[Conclusions](#)[References](#)[Tables](#)[Figures](#)[Back](#)[Close](#)[Full Screen / Esc](#)[Printer-friendly Version](#)[Interactive Discussion](#)

We define SM_{long} by fitting Eq. (1) to the soil moisture time series using the harmonic frequencies lower than 1 yr^{-1} that divide into the number of years in the data record (i.e., for $k/n = 1/m, 2/m, 3/m \dots (m-1)/m$, where m is the time series length in years). Finally, we define SM_{short} as the residual:

$$SM_{short} = SM - \langle SM \rangle - SM_{long} - SM_{seas} \quad (2)$$

where $\langle SM \rangle$ is the temporal mean soil moisture. Note that, as defined here, SM_{long} , SM_{seas} , and SM_{short} are all zero-mean, since the time series mean was assigned to a_0 in Eq. (1). The coverage statistics for each data set in Table 2 highlight that the AMSR-E and ARS observed time series are incomplete. When applied to incomplete time series, the sinusoids fitted by Eq. (1) are no longer necessarily independent, hence the fitted SM_{seas} and SM_{long} may not be independent. We opted not to use gap-filling prior to fitting Eq. (1), to keep the method simple, and because gap-filling would directly affect the SM_{short} dynamics. In Sect. 3, before using the decomposed time series we check for signs of strong dependence between the fitted SM_{long} , SM_{seas} , and SM_{short} , by testing whether the sum of the variances of the three time scale components differs from the variance of the original soil moisture time series. We assume that if there is no difference (or little difference) then any dependence between SM_{long} , SM_{seas} , and SM_{short} has only a minimal impact on our results. Following initial investigation with this test, the number of observations used at each location is maximized by comparing only model (or assimilation) estimates to ARS in situ measurements, avoiding direct comparison of the incomplete ARS and AMSR-E time series (which would require cross-screening for the availability of both). Finally, we do not use the harmonic fit to interpolate missing data, and instead screen out the fitted SM_{long} and SM_{seas} at times when the original soil moisture was not available. Also, at Reynolds Creek, where the time series has been truncated to remove frozen winters, the length of the year used to fit the harmonics was similarly truncated.

For demonstration purposes, we have also decomposed each soil moisture time series into similarly defined time scale components using moving averages, since mov-

Soil moisture
assimilation time
scales

C. Draper and R. Reichle

Title Page

Abstract

Introduction

Conclusions

References

Tables

Figures



Back

Close

Full Screen / Esc

Printer-friendly Version

Interactive Discussion



ing averages are often used for calculating anomaly correlations (Draper et al., 2012; Dorigo et al., 2015). The length of the averaging windows were chosen to give close agreement with the results of the harmonic decomposition described above. For the moving average decomposition, the inter-annual soil moisture time series, SM_{long}^{MA} , is defined as the 181 day moving average, and the seasonal cycle, SM_{seas}^{MA} , is defined for each day of the year by averaging the data from all years that fall within a 45 day window surrounding that day-of-year. As with the harmonic approach, the subseasonal time series, SM_{short}^{MA} , is calculated as the residual, analogous to Eq. (2). The same data processing and quality control as for the harmonic decomposition is used, plus the moving averages are only calculated when at least 60 % of the data within the averaging window are available.

3 Results

Below, the original AMSR-E, Catchment, and ARS soil moisture time series are examined (Sect. 3.1), before being split into SM_{seas} , SM_{long} , and SM_{short} (Sect. 3.2). The distribution of variance across the different time scales for each soil moisture estimate is then compared (Sect. 3.3), before the observations are rescaled (Sect. 3.4), and the benefit of assimilating the AMSR-E data into Catchment is assessed at each time scale (Sect. 3.5). Finally, the consequences of using a relatively short record to rescale the AMSR-E data is examined (Sect. 3.6).

3.1 The ARS, AMSR-E, and catchment time series

Figure 1 shows the original time series at each site. In general, soil moisture from in situ, modeled, and remotely sensed estimates have systematic differences in their behavior, due to representativity or structural differences between each estimate (Reichle et al., 2004). These systematic differences are clear in Fig. 1. The most obvious difference is that the mean and variance of each estimate differ (see also Table 2). Both

Title Page

Abstract

Introduction

Conclusions

References

Tables

Figures



Back

Close

Full Screen / Esc

Printer-friendly Version

Interactive Discussion



AMSR-E and Catchment are consistently biased high compared to the ARS soil moisture. Bias values for the model range from $0.01 \text{ m}^3 \text{ m}^{-3}$ for Little Washita to $0.09 \text{ m}^3 \text{ m}^{-3}$ for Little River, and bias values for the AMSR-E retrievals range from $0.07 \text{ m}^3 \text{ m}^{-3}$ for Reynolds Creek to $0.21 \text{ m}^3 \text{ m}^{-3}$ for Little River. Additionally, the standard deviation of AMSR-E is two to three times larger than the other two estimates. Figure 1 demonstrates that this is due to greater noise, and also a prominent seasonal cycle at Little Washita and Little River that is not evident in the other time series.

In addition to the systematic differences in their mean and standard deviation reported above, there are more subtle differences between the soil moisture dynamics described by each estimate. For example, for both the surface and root-zone soil moisture, the ARS time series tend to show a sharper response to individual rain events than does Catchment, with (relatively) larger peaks followed by more rapid dry down after each event. At Walnut Gulch this is particularly obvious, with ARS rapidly drying to a well defined lower limit after each precipitation event, while Catchment has a lesser response to individual events, and a stronger seasonal signal.

3.2 Soil moisture time series at each time scale

Figure 2 shows an example of the time scale decomposition, for the Catchment surface soil moisture at Little River, for both the harmonic and moving average approaches. The time series described by each method are similar in terms of the magnitude and timing of their dynamics, except that the moving average inter-annual soil moisture includes more high-frequency variability than does the harmonic version. Evaluation of soil moisture at specific time scales should ideally be based on time series separated into independent time scale components. For the harmonic method, independence between the time series at each time scale is not guaranteed since the original time series were not complete, while for the moving average method, independence is not expected.

Figure 3 shows an example of the variance bar plots used to check for signs of dependence between the time series at each time scale, in this case for the Catchment

Soil moisture assimilation time scales

C. Draper and R. Reichle

Title Page

Abstract

Introduction

Conclusions

References

Tables

Figures



Back

Close

Full Screen / Esc

Printer-friendly Version

Interactive Discussion



model and the AMSR-E observations. In Fig. 3a, for the harmonic method, the sum of the variances at each time scale (the stacked bars) is very close (within 2%) to the total variance of the original soil moisture time series (the white circles), falling within the 95% confidence interval of the total variance in each case. In contrast, for the moving average method in Fig. 3b the sum of the variances of each time scale falls outside the 95% confidence interval for the total time series variance at three of four sites, with a mean difference of 8% of the total variance (with differences ranging between 1 and 16%), indicating strong dependence between the three components. The sum of the variances of the time scale components is less than the total variance at each site, indicating positively correlated features between the moving average time scale components (since $\langle(\sigma_{X+Y}^2)\rangle = \langle\sigma_X^2\rangle - 2\langle\sigma_{XY}\rangle + \langle\sigma_Y^2\rangle$). This positive correlation is intuitively expected, since an anomaly in the original soil moisture time series has the same direction of influence on both the moving averages and the residual from that moving average (e.g., in Fig. 2 note the signal of the large positive anomaly in early 2004 in both $SM_{\text{long}}^{\text{MA}}$ and $SM_{\text{short}}^{\text{MA}}$). Finally, the distribution of variance across the time scales is similar for each method, largely because the moving average window lengths for $SM_{\text{seas}}^{\text{MA}}$ and $SM_{\text{long}}^{\text{MA}}$ were selected to generate time series closely matching those from the harmonic method.

3.3 Variance distribution across time scales

In Fig. 3 the AMSR-E variance is much larger than that for Catchment (as was discussed in Sect. 3.1), making it difficult to compare the relative distribution of variance across each time scale. Figure 4a then shows the AMSR-E and Catchment variance bar plots with the total variance normalized to one, to allow direct comparison to the fraction of variance at each time scale. The same plots are also presented for the Catchment and ARS soil moisture in Fig. 4b (recall we do not directly compare the ARS and AMSR-E time series, so as to avoid cross-screening their availability).

In Fig. 4, the distribution of variance across time scales for each data set can be very different, and there is not a consistent pattern across the four sites. As was previously

**Soil moisture
assimilation time
scales**

C. Draper and R. Reichle

Title Page	
Abstract	Introduction
Conclusions	References
Tables	Figures
⏪	⏩
⏴	⏵
Back	Close
Full Screen / Esc	
Printer-friendly Version	
Interactive Discussion	



Soil moisture assimilation time scales

C. Draper and R. Reichle

Title Page

Abstract

Introduction

Conclusions

References

Tables

Figures



Back

Close

Full Screen / Esc

Printer-friendly Version

Interactive Discussion



noted from Fig. 1, AMSR-E has a very prominent seasonal cycle at Little River and Little Washita (40–70 % of the total variance) that is not present for Catchment or ARS, for which the SM_{seas} fraction of variance is around 10–20 % in Fig. 4. In contrast, at Reynolds Creek and Walnut Gulch, Catchment has a larger fraction of its variance in the seasonal cycle (55–70 %) than does AMSR-E (20–40 %), with ARS agreeing with Catchment at Reynolds Creek only. At Walnut Gulch the greater variance-fraction in the Catchment SM_{seas} is mostly balanced by less variability in SM_{short} (30 % compared to 60 % for ARS). This is associated with the differing responses to precipitation events already noted in Fig. 2.

AMSR-E could be expected a priori to have a larger fraction of variance at SM_{short} , due to measurement noise in the remotely sensed observations. However, this is only the case at Reynolds Creek, where AMSR-E has 50 % of its variance in SM_{short} , compared to 20–30 % for Catchment and ARS. At Walnut Gulch, the AMSR-E and ARS SM_{short} variance-fractions are similar (50–60 %), while the fraction for Catchment is much lower (25 %). At Little Washita and Little River the variance-fraction in the AMSR-E SM_{short} is similar to Catchment (at around 50 and 30 %, respectively) and both are much smaller than for ARS (around 70 %). At these two sites the AMSR-E SM_{short} variance-fraction may be less than expected due to the large amount of variance in its exaggerated seasonal cycle.

For the SM_{long} variance, the patterns at Little Washita and Little River are again similar to each other. Catchment has much more variance in SM_{long} (40–50 %) than ARS (20 %) or AMSR-E (10 % or less). At the other two sites, the SM_{long} variance-fraction is similar for all data sets, except for the lower value for AMSR-E at Walnut Gulch (< 10 %, compared to around 20 % for ARS and Catchment).

3.4 Baseline observation rescaling

The systematic differences between observed and forecast soil moisture mean and variance (Fig. 3) motivate the practice of rescaling observations to match the model forecast climatology prior to assimilation. If this is not done, the assimilation may force

the model into a regime that is incompatible with its assumed structure and parameters, leading to degraded flux forecasts (De Lannoy et al., 2007). For the baseline experiment, the AMSR-E observations were rescaled using bulk CDF-matching parameters estimated over the full data record. By design, the CDF-matched AMSR-E observations, labeled Oc, have the same mean (not shown) and variance (Fig. 3a) as the Catchment soil moisture. Figure 4 shows that the CDF-matching had little impact on the variance distributions across each time scale. This suggests that for the examples in this study, the CDF-matching operator could be approximated by a linear rescaling, in which only the mean and variance of the model are matched, as in Scipal et al. (2008). Hence, the observation rescaling, and assimilation of the resulting observations, was repeated using linear rescaling of the AMSR-E observations in place of CDF-matching, with very similar results in terms of the rescaled observations and the assimilation output (for both the Oc rescaling presented here, and the Oy rescaling in Sect. 3.6).

Recall that the distribution of the variance across different time scales was quite different for AMSR-E and Catchment soil moisture in Fig. 4. Note that large errors in the variance at one time scale (in either AMSR-E or Catchment) will affect the rescaling of the variance at other time scales. In particular, if the unrealistically large AMSR-E seasonal cycle at Little Washita were replaced with something more realistic, for example representing 8% of the total variance (as in the ARS time series), then the fraction of variance in SM_{short} would increase from the current 48 to 75%, increasing the SM_{short} variance in the CDF-matched AMSR-E from 0.0036 to 0.0054 ($\text{m}^3 \text{m}^{-3}$)².

3.5 Evaluation of the baseline assimilation experiment at each time scale

The improvement gained from assimilating the AMSR-E observations is evaluated using the unbiased Mean Square Error (ubMSE) of the resulting model soil moisture, with respect to the ARS in situ observations. We define the ubMSE as the mean square difference after removing the long-term mean bias from both data sets. This is the square of the commonly used unbiased *root* mean square error (Entekhabi et al., 2010b). We

Soil moisture assimilation time scales

C. Draper and R. Reichle

Title Page

Abstract

Introduction

Conclusions

References

Tables

Figures



Back

Close

Full Screen / Esc

Printer-friendly Version

Interactive Discussion



do not use the square root to take advantage of the additive property of the variance of independent time series, however to aid interpretation the ubMSE equivalent to the common ubRMSE target accuracy of $0.04 \text{ m}^3 \text{ m}^{-3}$ is indicated in the relevant plots.

Figure 5 shows the ubMSE for each assimilation experiment, separated into each time scale. In the baseline assimilation experiment, labeled Ac, the observations CDF-matched over the full time period (Oc) were assimilated into the Catchment model. Prior to assimilation, the average ubMSE in the near-surface soil moisture across the four sites was $1.8 \times 10^{-3} (\text{m}^3 \text{ m}^{-3})^2$ (giving a ubRMSE just above the $0.04 \text{ m}^3 \text{ m}^{-3}$ target). Close to half (55%) of the ubMSE is in SM_{short} , with the rest split between SM_{seas} (26%) and SM_{long} (19%). The Ac assimilation significantly reduced the total ubMSE at each site, reducing the average near-surface ubMSE across the four sites by 33% to $1.2 \times 10^{-3} (\text{m}^3 \text{ m}^{-3})^2$, with average reductions in the near-surface layer of 52% for SM_{long} , 25% for SM_{seas} , and 22% for SM_{short} . The total ubMSE was reduced at each site for all time scale components, except for SM_{seas} at Little Washita (where the model ubMSE was already relatively small).

Root-zone soil moisture observations were available for the study period only at Little River. Both the distribution of the ubMSE across each time scale, and the relative reductions achieved from assimilation, are similar for the near-surface and root-zone layers at Little River in Fig. 5d and e, adding confidence that the model improvements reported above for the near-surface soil moisture are indicative of the performance throughout the soil profile.

To illustrate the impact of the assimilation at each time scale, Fig. 6 compares the decomposed time series for the Catchment model and Ac assimilation experiments to that from the ARS in situ observations at Little Washita. The difference between the three SM_{short} time series is difficult to visually judge in Fig. 6d, however, the impact of the assimilation on the SM_{seas} and SM_{long} time series is clear. Figure 6b suggests that the large SM_{long} ubMSE reduction (by over 80%) from the assimilation is due to the reduced amplitude in the SM_{long} dynamics, although there is perhaps also an improvement in event timing. In Fig. 6c, the model seasonal cycle has an overestimated

HESSD

12, 7971–8004, 2015

Soil moisture assimilation time scales

C. Draper and R. Reichle

Title Page

Abstract

Introduction

Conclusions

References

Tables

Figures

⏪

⏩

◀

▶

Back

Close

Full Screen / Esc

Printer-friendly Version

Interactive Discussion



amplitude, and also includes two maxima per year, where the ARS seasonal cycle has only one. The assimilation exacerbates the overestimated amplitude, but also removes the second annual maxima, resulting in an overall SM_{seas} ubMSE reduction (by 46 %).

3.6 Observation rescaling with a short data record

5 The nine year AMSR-E data record used here is the longest remotely sensed soil moisture record available from a single satellite sensor, and soil moisture assimilation experiments using newer satellites are limited to shorter time periods. Obviously, assimilating a shorter time period will limit the potential improvements to the model SM_{long} (of similar magnitude to the SM_{short} improvement in this study). The potential benefit
10 of an assimilation over a shorter period may also be limited by the increased sampling uncertainty in the estimated observation rescaling parameters. This increased uncertainty could arise from systematic errors due to inadequate sampling of SM_{seas} and SM_{long} , or from increased random errors associated with the smaller sample size. To establish the potential consequences of this uncertainty, we conducted nine additional
15 experiments, labeled A_y , with the rescaling parameters for each estimated from a 12 month period starting in consecutive Octobers (but assimilating the full eight or nine year near-surface soil moisture data record listed in Table 1).

In contrast to Reichle and Koster (2004), we do not use ergodic substitution (of spatial sampling for temporal sampling) when estimating the rescaling parameters with
20 a single year of observations, since with more modern remotely sensed data sets (than the SMMR data used by Reichle and Koster, 2004) this is no longer necessary to obtain a sufficient sample size. Additionally, for the assimilation of Soil Moisture Ocean Salinity retrievals, De Lannoy and Reichle (2015) found ergodic substitution degraded the estimated CDFs, by introducing conflicting information from neighboring grid cells
25 (possibly due to the higher spatial resolution, compared to SMMR).

The potential uncertainty introduced by using a single year to estimate the rescaling parameters depends on the inter-annual variability in the systematic differences between the observed and forecast soil moisture. The main systematic differences that

[Title Page](#)

[Abstract](#)

[Introduction](#)

[Conclusions](#)

[References](#)

[Tables](#)

[Figures](#)



[Back](#)

[Close](#)

[Full Screen / Esc](#)

[Printer-friendly Version](#)

[Interactive Discussion](#)



are addressed by the CDF-matching are the differences in the observed and forecast mean and standard deviation. For demonstrative purposes, Fig. 7 illustrates the difference between the means, and the ratio of the standard deviations, estimated using the full data record, and using each single year. In Fig. 7a there is considerable inter-annual scatter in the yearly mean differences, although by linearity the average is unbiased. The standard deviation ratio in Fig. 7b also shows inter-annual variability, however the single year ratios are also biased low compared to the all-years ratio, since the single year estimates did not sample the SM_{long} variance (which was consistently a greater fraction of the total variance for Catchment than for AMSR-E in Fig. 4a). This is particularly marked at Little River, where the average of the single year standard deviation ratios was 30 % less than when estimated using all years (since SM_{long} makes up close to 50 % of the total variance in Catchment, compared to less than 5 % for AMSR-E in Fig. 4a).

Figure 5 includes the ubMSE for the nine Ay assimilation experiments, as well as the mean ubMSE ($\langle Ay \rangle$) across all nine. Note that errors in the rescaling of the mean value are likely under-reported here, since any introduction of biases into the model will not be directly detected by the ubMSE. Comparing the 35 individual Ay experiments to the baseline Ac experiments, most of the Ay experiments resulted in larger total ubMSE than the Ac experiment did at Reynolds Creek, Walnut Gulch, and Little Washita, while the opposite occurred at Little River. Overall there were eight Ay experiments for which the total ubMSE was significantly different (at the 5 % level) and higher than for the Ac experiment, seven for which it was significantly different and lower, and 20 where the ubMSE was not significantly changed. The differences between the Ac and Ay ubMSE are skewed, in that when the Ay ubMSE is higher, the difference tends to be greater than when it is lower. Consequently, the average reduction in the model ubMSE for the near-surface soil moisture, compared to the model with no assimilation, is slightly less for $\langle Ay \rangle$ (30 %) than for Ac (33 %).

Each instance of relatively poor ubMSE for an Ay experiment can be traced to the more extreme (i.e., unrepresentative) single year systematic differences in Fig. 7. For

Soil moisture assimilation time scales

C. Draper and R. Reichle

[Title Page](#)[Abstract](#)[Introduction](#)[Conclusions](#)[References](#)[Tables](#)[Figures](#)[Back](#)[Close](#)[Full Screen / Esc](#)[Printer-friendly Version](#)[Interactive Discussion](#)

example, going through the experiments with the largest relative increase in ubMSE, experiment Ay07 at Reynolds Creek, and experiments Ay05, Ay06, and Ay07 at Walnut Gulch all have extreme standard deviation ratios, while Ay06 at Reynolds Creek and Ay10 at Little Washita have extreme mean differences. In each case, most of the increase in the ubMSE is due to increased errors in the SM_{seas} and SM_{long} components, suggesting that the SM_{short} corrections are more robust to uncertainty in the scaling parameters. The result that unrepresentative mean difference corrections can impact the ubMSE (a bias-robust metric) is interesting in that it demonstrates that bias-free assimilation of biased observations can degrade model soil moisture dynamics. Note also that unrepresentative scaling parameters do not necessarily degrade the assimilation output, and in some instances are even advantageous. Most obviously, at Little River, where the single year standard deviation ratios were biased low (by 30%), the Ay assimilation experiments all produced slightly lower ubMSE than the Ac experiment.

Above, the assimilation of AMSR-E data that has been rescaled using parameters estimated from a single year, and from the full time period were compared, showing that the average ubMSE is slightly higher when the single year parameters were used. However, it is perhaps more relevant to assess whether the assimilation is still beneficial when the single year parameters are used. Figure 5 suggests that on average it is. As with the Ac experiment, the $\langle Ay \rangle$ ubMSE is consistently less than that of the model at all time scales, except for SM_{seas} at Little Washita. However, for individual realizations there is an increased risk when using the single year parameters that the assimilation will not significantly improve the model, or will even significantly degrade the model. For example, at Little Washita, where the Ac experiment reduced the ubMSE by a small but significant amount, none of the Ay experiments significantly decreased the ubMSE, and the Ay10 experiment significantly significantly increased it.

HESSD

12, 7971–8004, 2015

Soil moisture assimilation time scales

C. Draper and R. Reichle

Title Page

Abstract

Introduction

Conclusions

References

Tables

Figures



Back

Close

Full Screen / Esc

Printer-friendly Version

Interactive Discussion



that the model would benefit from correcting this error, in terms of improvements to forecast skill.

Assimilating the AMSR-E observations also reduced the near-surface SM_{seas} ubMSE by 26%, averaged across the four sites, suggesting the possibility that the assimilation was beneficial to the modeled mean seasonal cycle, despite not being designed to address systematic errors. However, even more so than for SM_{long} , the reduced SM_{seas} ubMSE could be due to reduced representativity differences, rather than a genuine improvement to the model's ability to represent the desired physical processes. To confirm that the SM_{long} and SM_{seas} ubMSE reductions do indicate improved model soil moisture would require evaluating the dependent moisture and energy flux forecast, and unfortunately verifying observations are not available at the study locations.

In comparing the AMSR-E and Catchment soil moisture at each time scale in this study, it became apparent that the distribution of variance across each time scale was very different between the remotely sensed and modeled soil moisture time series (Fig. 4). Traditionally, observation rescaling strategies used in land data assimilation do not distinguish between variability at different time scales, and apply a single set of bulk rescaling parameters to the full time series. Consequently, the large discrepancies in the variance at one time scale (due to errors in one of or both estimates) can have follow-on effects for the rescaling of other time scales. For example, the unrealistically large AMSR-E seasonal cycle at Little Washita caused the variability at SM_{long} and SM_{short} to be overly dampened in this study. This could perhaps be avoided by using rescaling methods that rescale each time scale separately (e.g., Su and Ryu, 2015).

In addition to observation bias removal strategies that respect the time scale-dependent nature of observation – forecast systematic differences, it may be advantageous to target only certain time scales, for example by retaining the model seasonal cycle while rescaling other time scales (e.g., Bolten et al., 2010; Yilmaz et al., 2015). Ultimately, whether these approaches will be beneficial will depend on whether the model observation differences at each time scale are caused by model or observation

HESSD

12, 7971–8004, 2015

Soil moisture assimilation time scales

C. Draper and R. Reichle

Title Page

Abstract

Introduction

Conclusions

References

Tables

Figures

⏪

⏩

◀

▶

Back

Close

Full Screen / Esc

Printer-friendly Version

Interactive Discussion



the single year parameters was small, and did not practically reduce the benefit gained from the assimilation.

Acknowledgements. Thanks to Balachandrudu Narapusetty for helpful comments, USDA-ARS and Michael Cosh for providing access to the long term in situ soil moisture observations from the experimental watersheds. The AMSR-E soil moisture retrievals were obtained from the NASA Goddard Earth Sciences Data and Information Services Center (GES DISC). This work was supported by the NASA Terrestrial Hydrology program (NNX15AB52G).

References

- Bolten, J., Crow, W., Zhan, X., Jackson, T., and Reynolds, C.: Evaluating the utility of remotely sensed soil moisture retrievals for operational agricultural drought monitoring, *IEEE J. Sel. Top. Appl.*, 3, 57–66, doi:10.1109/JSTARS.2009.2037163, 2010. 7973, 7974
- De Lannoy, G. and Reichle, R.: Global assimilation of multi-angular SMOS brightness temperature observations into the GEOS-5 Catchment land surface model for soil moisture estimation, *IEEE T. Geosci. Remote*, submitted, 2015. 7987
- De Lannoy, G., Reichle, R., Houser, P., Pauwels, V., and Verhoest, N.: Correcting for forecast bias in soil moisture assimilation with the ensemble Kalman filter, *Water Resour. Res.*, 43, W09410, doi:10.1029/2006WR005449, 2007. 7985
- De Lannoy, G., Koster, R., Reichle, R., Mahanama, S., and Liu, Q.: An updated treatment of soil texture and associated hydraulic properties in a global land modeling system, *J. Adv. Model. Earth Syst.*, 6, 957–979, doi:10.1002/2014MS000330, 2014. 7977
- Dorigo, W., Gruber, A., de Jeu, R., Wagner, W., Stacke, T., Loew, A., Albergel, C., Brocca, L., Chung, D., Parinussa, R., and Kidd, R.: Evaluation of the ESA CCI soil moisture product using ground-based observations, *Remote Sens. Environ.*, 162, 380–395, doi:10.1016/j.rse.2014.07.023, 2015. 7981
- Draper, C., Reichle, R., De Lannoy, G., and Liu, Q.: Assimilation of passive and active microwave soil moisture retrievals, *Geophys. Res. Lett.*, 39, L04401, doi:10.1029/2011GL050655, 2012. 7973, 7981, 7990
- Drusch, M., Wood, E., and Gao, H.: Observation operators for the direct assimilation of TRMM microwave imager retrieved soil moisture, *Geophys. Res. Lett.*, 32, L15403, doi:10.1029/2005GL023623, 2005. 7974

Soil moisture assimilation time scales

C. Draper and R. Reichle

Title Page

Abstract

Introduction

Conclusions

References

Tables

Figures



Back

Close

Full Screen / Esc

Printer-friendly Version

Interactive Discussion



Soil moisture assimilation time scales

C. Draper and R. Reichle

Title Page

Abstract

Introduction

Conclusions

References

Tables

Figures



Back

Close

Full Screen / Esc

Printer-friendly Version

Interactive Discussion



Entekhabi, D., Njoku, E., O'Neill, P., Kellogg, K., Crow, W., Edelstein, W., Entin, J., Goodman, S., Jackson, T., Johnson, J., Kimball, J., Piepmeier, J., Koster, R., Martin, N., McDonald, K., Moghaddam, M., Moran, S., Reichle, R., Shi, J., Spencer, M., Thurman, S., Tsang, L., and Van Zyl, J.: The Soil Moisture Active Passive (SMAP) mission, P. IEEE, 98, 704–716, doi:10.1109/jproc.2010.2043918, 2010a. 7976

Entekhabi, D., Reichle, R., Koster, R., and Crow, W.: Performance metrics for soil moisture retrievals and application requirements, J. Hydrometeorol., 11, 832–840, doi:10.1175/2010JHM1223.1, 2010b. 7975, 7985

Entin, J., Robock, A., Vinnikov, K., Hollinger, S., Liu, S., and Namkhai, A.: Temporal and spatial scales of observed soil moisture variations in the extratropics, J. Geophys. Res., 105, 11865–11877, doi:10.1029/2000JD900051, 2000. 7974

Jackson, T., Cosh, M., Bindlish, R., Starks, P., Bosch, D., Seyfried, M., Goodrich, D., Moran, M., and Du, J.: Validation of advanced microwave scanning radiometer soil moisture products, IEEE T. Geosci. Remote, 48, 4256–4272, doi:10.1109/TGRS.2010.2051035, 2010.

Koster, R., Suarez, M., Ducharne, A., Stieglitz, M., and Kumar, P.: A catchment-based approach to modeling land surface processes in a general circulation model: 1. Model structure, J. Geophys. Res., 105, 24809–24822, doi:10.1029/2000JD900327, 2000. 7976

Liu, Q., Reichle, R., Bindlish, R., Cosh, M., Crow, W., de Jeu, R., De Lannoy, G., Huffman, G., and Jackson, T.: The contributions of precipitation and soil moisture observations to the skill of soil moisture estimates in a land data assimilation system, J. Hydrometeorol., 12, 750–765, doi:10.1175/JHM-D-10-05000.1, 2011. 7978

Narapusetty, B., DelSole, T., and Tippet, M.: Optimal estimation of the climatological mean, J. Climate, 22, 4845–4859, doi:10.1175/2009JCLI2944.1, 2009. 7979

Owe, M., de Jeu, R., and Holmes, T.: Multisensor historical climatology of satellite-derived global land surface moisture, J. Geophys. Res., 113, F01002, doi:10.1029/2007JF000769, 2008.

Reichle, R. and Koster, R.: Bias reduction in short records of satellite soil moisture, Geophys. Res. Lett., 31, L19501, doi:10.1029/2004GL020938, 2004. 7973, 7975, 7978, 7987, 7992

Reichle, R., Koster, R., Dong, J., and Berg, A.: Global soil moisture from satellite observations, land surface models, and ground data: implications for data assimilation, J. Hydrometeorol., 5, 430–442, doi:10.1175/1525-7541(2004)005<0430:GSMFSO>2.0.CO;2, 2004. 7981

Reichle, R., Koster, R., Liu, P., Mahanama, S., Njoku, E., and Owe, M.: Comparison and assimilation of global soil moisture retrievals from the Advanced Microwave Scanning Radiometer

Soil moisture assimilation time scales

C. Draper and R. Reichle

Title Page

Abstract

Introduction

Conclusions

References

Tables

Figures



Back

Close

Full Screen / Esc

Printer-friendly Version

Interactive Discussion



for the Earth Observing System (AMSR-E) and the Scanning Multichannel Microwave Radiometer (SMMR), *J. Geophys. Res.*, 112, D09108, doi:10.1029/2006JD008033, 2007. 7973, 7990

5 Rienecker, M., Suarez, M., Gelaro, R., Todling, R., Bacmeister, J., Liu, E., Bosilovich, M., Schubert, S., Takacs, L., Kim, G.-K., Bloom, S., Chen, J., Collins, D., Conaty, A., da Silva, A., Gu, W., Joiner, J., Koster, R., Lucchesi, R., Molod, A., Owens, T., Pawson, S., Pegion, P., Redder, C., Reichle, R., Robertson, F., Ruddick, A., Sienkiewicz, M., and Woollen, J.: MERRA – NASA's Modern-Era Retrospective Analysis for Research and Applications, *J. Climate*, 24, 3624–3648, doi:10.1175/JCLI-D-11-00015.1, 2011.

10 Schaefer, G., Cosh, M., and Jackson, T.: The USDA Natural Resources Conservation Service Soil Climate Analysis Network (SCAN), *J. Atmos. Ocean. Tech.*, 24, 2073–2077, doi:10.1175/2007JTECHA930.1, 2007. 7977

Scharlemann, J., Benz, D., Hay, S., Purse, B., Tatem, A., Wint, G. W., and Rogers, D.: Global data for ecology and epidemiology: a novel algorithm for temporal fourier processing MODIS data, *PLOS ONE*, 1, e1408, doi:10.1371/journal.pone.0001408, 2008. 7979

15 Scipal, K., Drusch, M., and Wagner, W.: Assimilation of a ERS scatterometer derived soil moisture index in the ECMWF numerical weather prediction system, *Adv Water Resour*, 31, 1101–1112, doi:10.1016/j.advwatres.2008.04.013, 2008. 7973, 7985, 7990

Su, C.-H. and Ryu, D.: Multi-scale analysis of bias correction of soil moisture, *Hydrol. Earth Syst. Sci.*, 19, 17–31, doi:10.5194/hess-19-17-2015, 2015. 7974

20 Vinnikov, K., Yu, Y., Rama Varma Raja, M., Tarpley, D., and Goldberg, M.: Diurnal-seasonal and weather-related variations of land surface temperature observed from geostationary satellites, *Geophys. Res. Lett.*, 35, L22708, doi:10.1029/2008gl035759, 2008. 7979

Yilmaz, M., Crow, W., and Ryu, D.: Impact of model relative accuracy in framework of rescaling observations in hydrological data assimilation studies, *Water Resour. Res.*, submitted, 2015. 7974

Soil moisture
assimilation time
scales

C. Draper and R. Reichle

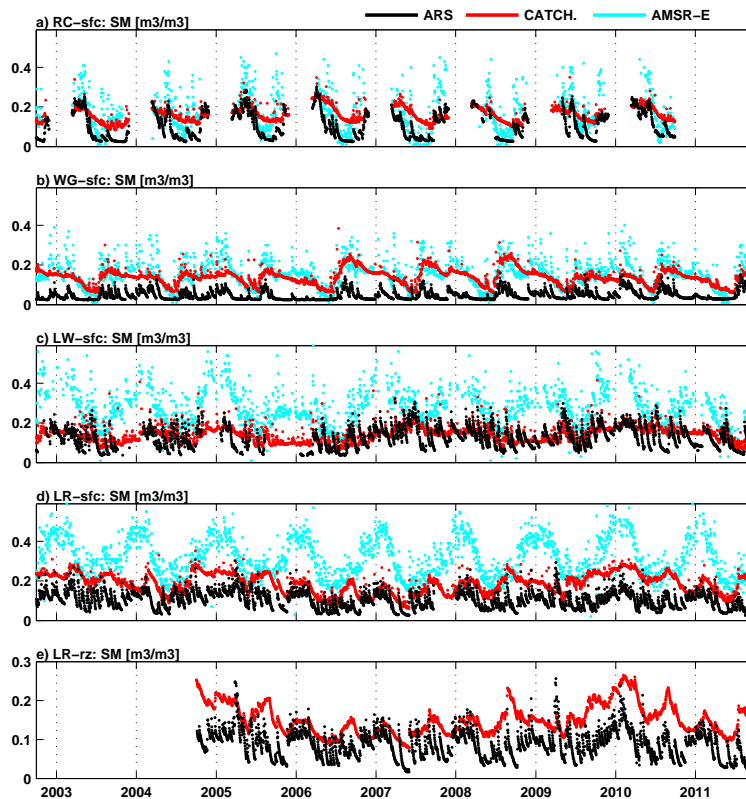


Figure 1. The ARS in situ, Catchment model, and AMSR-E remotely sensed surface soil moisture, with near-surface soil moisture at (a) Reynolds Creek, (b) Walnut Gulch, (c) Little Washita, (d) Little River, and (e) root-zone soil moisture at Little River.

[Title Page](#)[Abstract](#)[Introduction](#)[Conclusions](#)[References](#)[Tables](#)[Figures](#)[Back](#)[Close](#)[Full Screen / Esc](#)[Printer-friendly Version](#)[Interactive Discussion](#)

Soil moisture
assimilation time
scales

C. Draper and R. Reichle

Title Page

Abstract

Introduction

Conclusions

References

Tables

Figures

◀

▶

◀

▶

Back

Close

Full Screen / Esc

Printer-friendly Version

Interactive Discussion

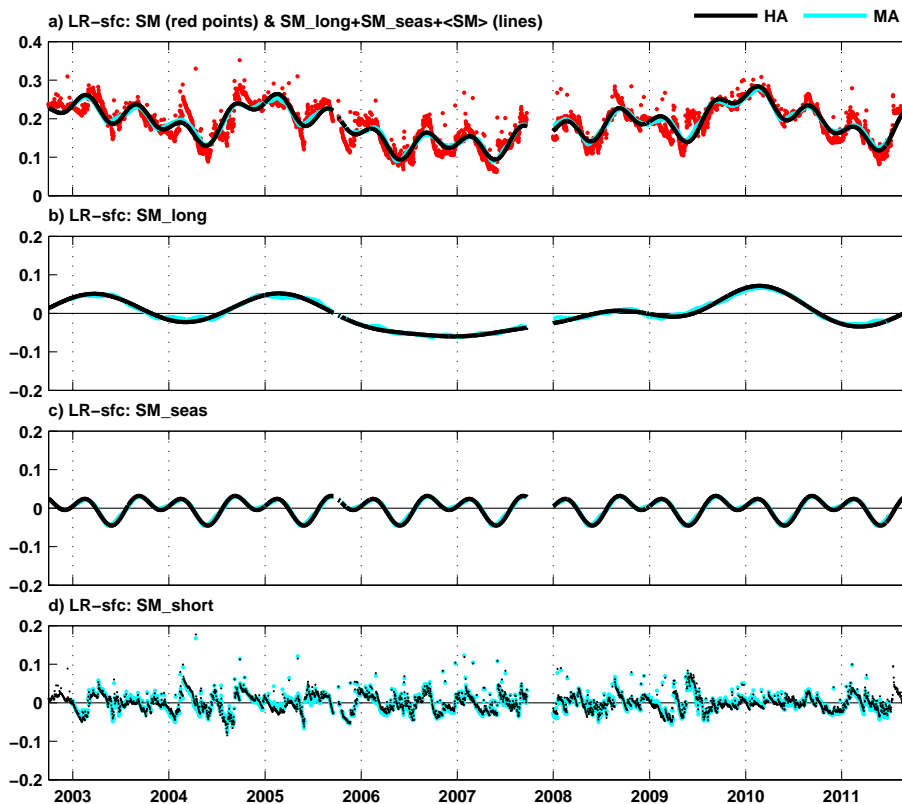


Figure 2. Decomposition of the Catchment near-surface soil moisture time series at Little River, using the harmonic (HA; black) and moving average (MA; cyan) methods, for **(a)** the original time series (red dots) and the sum of $SM_{long} + SM_{seas} +$ the long-term mean soil moisture (solid lines), and the individual components **(b)** SM_{long} , **(c)** SM_{seas} , and **(d)** SM_{short} .

Soil moisture assimilation time scales

C. Draper and R. Reichle

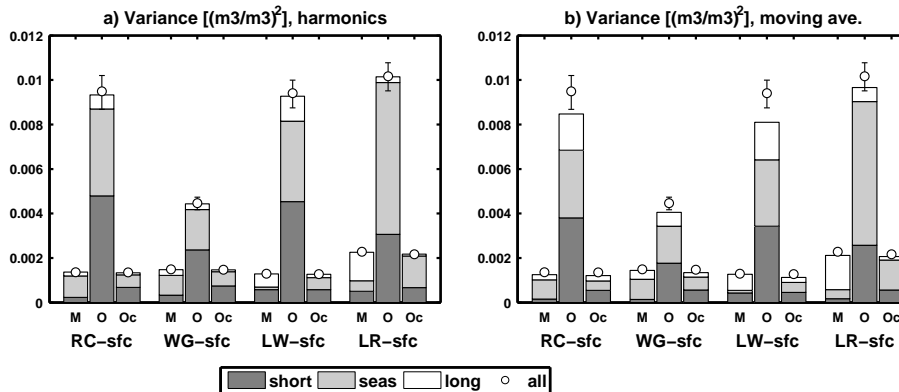


Figure 3. Time series variance at each time scale, with the Catchment Model (M), original AMSR-E Observed (O), and CDF-matched AMSR-E Observed (Oc) soil moisture variances plotted for the (a) harmonic, and (b) moving average decomposition methods. The circles and error bars give the variance of the original soil moisture time series, with 95% confidence intervals (some very small confidence intervals are obscured by the plotted circles).

Title Page

Abstract Introduction

Conclusions References

Tables Figures

◀ ▶

◀ ▶

Back Close

Full Screen / Esc

Printer-friendly Version

Interactive Discussion



Soil moisture assimilation time scales

C. Draper and R. Reichle

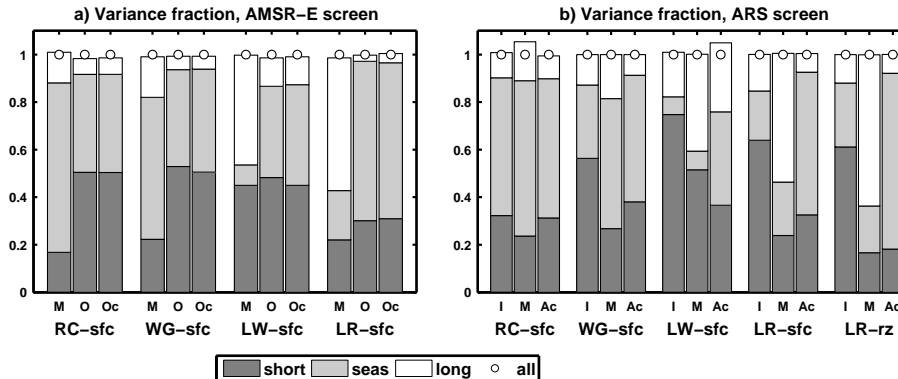


Figure 4. Fraction of variance at each time scale, obtained by normalizing the time series variance before decomposition. The Catchment Model (M), original AMSR-E Observed (O), and the CDF-matched AMSR-E Observed (Oc) soil moisture time series, cross-screened for AMSR-E availability, are plotted in (a), and the ARS In situ observations (I), Catchment model (M), and baseline assimilation (Ac) soil moisture time series, cross-screened for ARS availability, are plotted in (b). The circles give the variance of the original (normalized) soil moisture time series.

Title Page

Abstract

Introduction

Conclusions

References

Tables

Figures

⏪

⏩

◀

▶

Back

Close

Full Screen / Esc

Printer-friendly Version

Interactive Discussion



Soil moisture
assimilation time
scales

C. Draper and R. Reichle

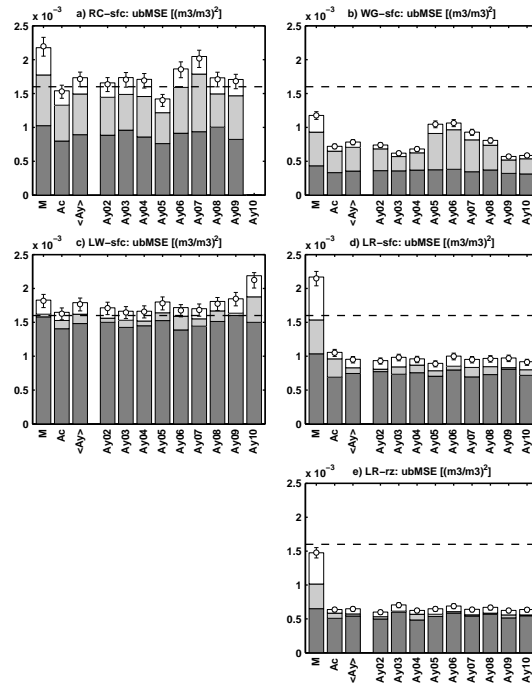


Figure 5. Error variances (ubMSE) compared to ARS in situ observations at each time scale, for the near-surface soil moisture at **(a)** Reynolds Creek, **(b)** Walnut Gulch, **(c)** Little Washita, **(d)** Little River, and **(e)** for the root-zone soil moisture at Little River. Bars show the Catchment model open loop (M), baseline assimilation (Ac), individual Ay assimilation experiments, and the mean across the Ay experiments ($\langle \text{Ay} \rangle$). Label AyYY indicates the Ay experiment with bias correction parameters estimated from the 12 months from 1 October of 20YY. Circles and error bars give the ubMSE and its 95 % confidence interval for the original soil moisture time series (some very small confidence intervals are obscured by the plotted circles). The dashed line at ubMSE of $1.6 \times 10^{-3} (\text{m}^3 \text{m}^{-3})^2$ is equivalent to the common ubRMSE target of $0.04 \text{ m}^3 \text{m}^{-3}$.

Soil moisture
assimilation time
scales

C. Draper and R. Reichle

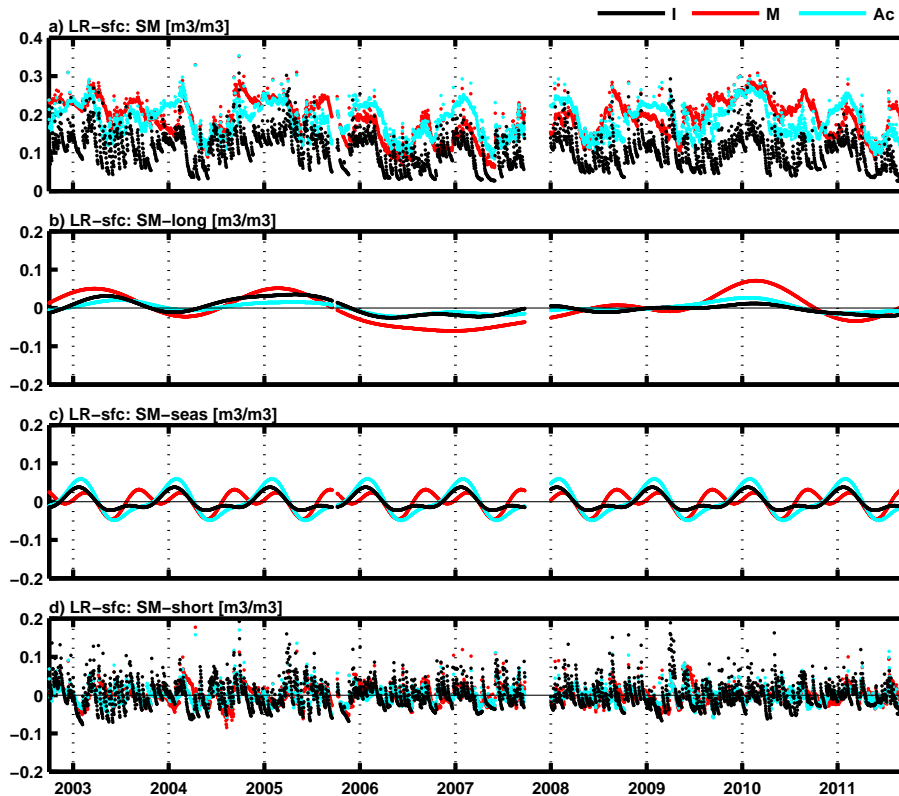


Figure 6. Decomposition of the ARS In situ (I), Catchment model (M), and baseline assimilation output (Ac) near-surface soil moisture time series at Little River, showing the (a) original time series, (b) SM_{long} , (c) SM_{seas} , and (d) SM_{short} .

Title Page

Abstract

Introduction

Conclusions

References

Tables

Figures

◀

▶

◀

▶

Back

Close

Full Screen / Esc

Printer-friendly Version

Interactive Discussion



Soil moisture assimilation time scales

C. Draper and R. Reichle

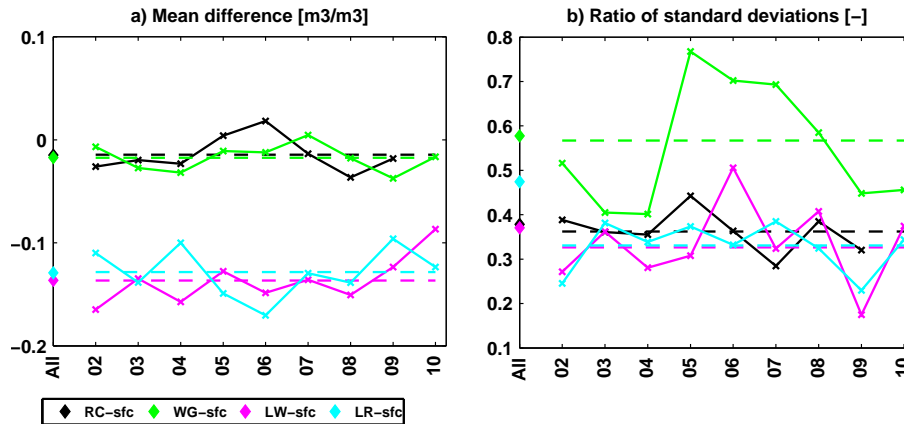


Figure 7. Systematic differences between AMSR-E observations and Catchment model near-surface soil moisture, with (a) the mean difference ($\langle \text{model} \rangle - \langle \text{observation} \rangle$), and (b) the ratio of the standard deviations ($\sigma(\text{model})/\sigma(\text{observations})$). The parameters are estimated using all years (All), and each year separately (with label YY indicating the parameters estimated from the 12 months from 1 October of 20YY), and the dashed lines give the mean of the YY parameters.